



HAL
open science

A study of the dependence on the Co and Ni proportions of the oxidation at elevated temperature of TaC-strengthened Ni and Co-based cast superalloys

Patrice Berthod, Jean-Paul Gomis, Ghouti Medjahdi, Pierre-Jean Panteix,
Lionel Aranda

► To cite this version:

Patrice Berthod, Jean-Paul Gomis, Ghouti Medjahdi, Pierre-Jean Panteix, Lionel Aranda. A study of the dependence on the Co and Ni proportions of the oxidation at elevated temperature of TaC-strengthened Ni and Co-based cast superalloys. *Materials Chemistry and Physics*, 2020, 251, pp.123088. 10.1016/j.matchemphys.2020.123088 . hal-03490439

HAL Id: hal-03490439

<https://hal.science/hal-03490439>

Submitted on 22 Aug 2022

HAL is a multi-disciplinary open access archive for the deposit and dissemination of scientific research documents, whether they are published or not. The documents may come from teaching and research institutions in France or abroad, or from public or private research centers.

L'archive ouverte pluridisciplinaire **HAL**, est destinée au dépôt et à la diffusion de documents scientifiques de niveau recherche, publiés ou non, émanant des établissements d'enseignement et de recherche français ou étrangers, des laboratoires publics ou privés.



Distributed under a Creative Commons Attribution - NonCommercial 4.0 International License

A study of the dependence on the Co and Ni proportions of the oxidation at elevated temperature of TaC-strengthened {Ni and Co}-based cast superalloys

Patrice Berthod, Jean-Paul Gomis,

Ghouthi Medjahdi, Pierre-Jean Panteix, Lionel Aranda

Institut Jean Lamour

*Department N°2: Chemistry and Physics of Solids and Surfaces
Team "Surface and interface, chemical reactivity of materials"
Campus ARTEM, 2 allée André Guinier - University of Lorraine
B.P. 50840, 54000 Nancy – France*

Corresponding author's e-mail: patrice.berthod@univ-lorraine.fr

Corresponding author's phone: (33)3 7274 2729

Abstract: Cobalt and nickel may play antagonist roles on the microstructures and high temperature properties of cast chromium-rich superalloys containing the same tantalum and carbon molar fractions. Since such alloys may be considered for uses at temperature levels as high as 1200°C, the whole range of base compositions was explored with six model quaternary alloys with Ni and Co contents varying from 0 to 100% of the remaining elements, the 25wt.%Cr, 0.4wt.%C and 6wt.%Ta being deducted. The interdendritic carbide network of the as-cast microstructures is made of chromium carbides and tantalum carbides for the Ni-richest alloys and of TaC only for the Co-richest ones. {170h, 1200°C}-exposure carried out in laboratory air led to important morphology deterioration for the two Ni-richest alloys but limited fragmentation of the TaC in the four Co-richest alloys. At the same time, the most of the alloys more or less well behaved in oxidation, except the two Co-richest alloys for which the too hindered volume diffusion of chromium did not sustain the chromia-forming behavior. Notably the Ni-free cobalt-based alloys suffered from starts of catastrophic oxidation in several surface locations. The quaternary alloy bases allowing taking benefit of the best compromise between hot oxidation resistance and possibly good mechanical behavior at elevated temperature was the model alloys with 14 to 28 wt.%Ni.

Keywords: alloys (A); solidification (B); electron microscopy (C); hardness (D); oxidation (D)

A study of the dependence on the Co and Ni proportions of the oxidation at elevated temperature of TaC-strengthened {Ni and Co}-based cast superalloys

1. Introduction

Even if advanced superalloys have appeared during the last decades (Directionally Solidified alloys, Single-Crystals, Oxide Dispersed Superalloys [1]), and recently alloys elaborated by additive manufacturing, conventionally cast superalloys stay very interesting for a not so low number of hot pieces. Owing to their coarse and randomly oriented grains, the equiaxed superalloys offer high level and isotropic mechanical properties at high temperature, which may be associated to the possibility to obtain complex shapes [2]. The alloys containing carbon and carbide-former elements may solidify with a dendritic structure, with possible strengthening of their grain boundaries and interdendritic spaces by eutectic carbides. Particularly interesting mechanical properties can be achieved when these carbides are very refractory and stable at high temperature as this is the case for many MC-type ones [3,4]. Among these carbides, tantalum carbides are of a great importance since, during equiaxed solidification, they crystallize as script-like eutectic carbides, and during long stays at high temperature they are more resistant than others (e.g. chromium carbides) to fragmentation, coalescence/coarsening [5]. Furthermore they favor high solidus temperature by comparison to chromium carbides; as example eutectics made of TaC and the matrix of a cobalt-based alloy melt about 40°C higher than the {chromium carbide; matrix} eutectic [6,7]. Tantalum carbides are used in polycrystalline cobalt-based alloys since a

long time, as in the famous Mar-M 509 superalloy [2] and derivatives [9-11]. If TaC carbides generally precipitate without problem at solidification in cobalt-based alloys [5-12], they can be also obtained in nickel-based alloys [13, 14] in which they may significantly influence the mechanical properties [15-17]. One can also meet these TaC carbides in directionally solidified alloys, based on nickel [18] as well as on cobalt [19], and also in cobalt alloys highly alloyed with rhenium [20, 21].

To optimize both the refractoriness and the TaC-reinforcement of conventionally cast superalloys rich in chromium for hot oxidation & corrosion purpose, it is compulsory to rate the Ta and C contents to prevent the appearance of chromium carbides (origin of solidus temperature lowering) and to obtain a TaC quantity high enough for efficiently strengthen the alloy but not too high to avoid possible lack of toughness and ductility. With a reasonable carbon content and by respecting the molar equivalence between tantalum and carbon, 0.4 wt.%C and 6wt.%Ta represent a good choice. When 30wt.%Cr are present in the alloys for favoring a chromia-forming behavior [22, 23], his metallurgical recipe does work for cobalt-based alloys [10, 6, 3] but not really for nickel-based ones [24]. Indeed the molar equivalence between Ta and C is enough to promote the formation of a strengthening carbides network only composed of TaC while the same Ta and C contents lead to a double population of interdendritic carbides, script-like eutectic TaC and acicular eutectic Cr₇C₃. Knowing that a Co-30Cr environment allows obtaining only TaC one can suppose that Co is a favorable element which can be interesting to add in partial replacement of Ni in nickel-chromium alloys. Furthermore, diminishing the chromium content – but not too much to keep a good oxidation and corrosion resistance at high temperature – can be also a solution to favor TaC in Ni-rich {cobalt & nickel}-based alloys.

In the present work the {25Cr, 0.4C, 6Ta} (wt.%) association of chromium, carbon and tantalum was considered, for all a series of alloys in which progressive addition of Co will be done, from an alloy only based on Co to an alloy only based on Ni. Alloys will be synthesized in small quantities by induction melting under inert atmosphere and the obtained as-cast microstructures will be examined. In a second time an exposure at an elevated temperature (1200°C) during rather long time (a whole week) will be performed in air to answer two questions: 1/are the as-cast microstructures stable on long time at high temperature? and 2/ how the Ni substitution by Co may influence the surface stability in oxidizing atmosphere? These questions are effectively important since the possible changes in natures, volume fractions and morphologies of the carbides on one hand, and the modification of Cr diffusion easiness on the second hand, both drive the sustainability of the alloys in real situation.

2. Material and methods

The alloys elaborated for this study are thus designed to be:

- * hot corrosion resistant to gases and melts but also to lower its competition with Ta in the carbides formation: 25wt.%Cr (value in the bottom of the range usually leading to a chromia-forming behavior)

- * to favor the TaC formation by respecting the molar equivalence between Ta and C, and to control the quantity of formed carbides for a good compromise between high strength at high temperature and acceptable toughness and ductility: 0.4 wt.%C and 6 wt.%Ta

* representative of the whole range of alloys existing between ones based on Ni only and ones based on Co only: for the remaining weight content (100-25-0.4-6 -> 68.6wt.%) to share between Ni and Co; total of six alloys containing, in wt.%: 68.6Ni-0Co (i.e. 0/5Co-5/5Ni), 54.9Ni-13.7Co (i.e. 1/5Co-4/5Ni) ... 0Ni-68.6Co (5/5Co-0/5Ni). These successive alloys were logically named “0Co5NiTa”, “1Co4NiTa” ... “5Co0NiTa”.

About 40g of each alloy was prepared as compact ingots by:

- Weighing, with a precision balance, the masses of pure elements (Ni, Co, C, Cr, Ta; Alfa Aesar; purity higher than 99.9wt.%)
- Melting each of the six alloys in a high frequency induction furnace under 300 milibars of argon, following a same procedure: 2 min achieve total melting, 5 min in the liquid state by maintaining the 110 kiloHertz – 4 kiloVolts applied parameters, about 1 min of solidification and 25 min of total cooling down to ambient temperature.

The following steps of sample preparation were (for each alloy):

- Ingots cut with a metallographical saw to obtain different parts
- Embedding in cold resin mixture (ESCIL), grinding with SiC papers under water (#240 to #1200-grit) and polishing (textile disk with 1µm abrasive particles) until obtaining a mirror-like state
- Grinding with #1200-grit SiC paper the surface of a part for the high temperature exposure

The different tests and observations which were carried out with these samples were:

- Characterization of the as-cast microstructure using a Scanning Electron Microscope (SEM: JEOL JSM6010-LA) in Back Scattered Electrons mode (BSE: 20kV of acceleration voltage, magnification ranging from $\times 250$ to $\times 250$) and of its Energy Dispersion Spectrometry (EDS) device
- Oxidation test in a box furnace for 170 hours (a week) at $1200 \pm 2^\circ\text{C}$, in laboratory air, all samples together but each per ceramic (alumina) shuttle, these shuttles being separated enough to avoid any contact between samples and to collect the eventually spalled of oxide without mix between alloys
- X-Ray Diffraction (XRD: Philips X'Pert Pro diffractometer) carried out on the spalled off oxides collected in the ceramic shuttles
- Embedding, cross-sectional cutting, grinding and polishing to obtain samples for metallographic characterization
- SEM/BSE and SEM/EDS characterization of the oxidized/aged alloys: oxides scales, internal oxides, sub-surface deterioration and microstructure changes in bulk
- Bulk hardness measurements for the as-cast and aged samples of each alloy by Vickers indentation under a 10kg-load (average and standard deviation values from up to 10 measurements).

3. Results

3.1. Real chemical compositions and initial microstructures of the six alloys

The first use of the embedded then polished samples of the as-cast alloys was to control their chemical compositions. Results of five full frame EDS analyses are given for each alloy in Table 1. Globally the wished contents in Co, Ni, Cr and Ta were successfully obtained. However one must notice the Ta values a little too high. This

overestimation is a usual phenomenon when EDS analyses are carried out on samples in which a significant part of Ta is contained in carbides. The carbon contents were not specified, since not possible by EDS for so low contents of this light element.

The microstructures of the six alloys are illustrated by SEM/BSE micrographs in Figure 1. All alloys are composed of a dendritic matrix, the interdendritic spaces being occupied by carbides. These later ones are of two types in the four nickel-richest alloys: chromium carbides (Cr_7C_3) and TaC. They are present in equivalent proportions in the 0Co5NiTa alloy, but the TaC proportion increases at the expense of the chromium carbides with the successive Co-enrichments until the 3Co2NiTa alloy in which TaC is clearly the major carbide phase. In the two cobalt-richest alloys, the carbides are exclusively, at least mainly, composed of tantalum carbides. By considering the morphologies of these chromium carbides and tantalum carbides, which are closely mixed with the periphery of the matrix dendrites, they are all of a eutectic nature. One can also notice that the total surface fractions of carbides are typical of 0.4wt.%C-containing alloy: the wished compositions were really reached.

3.2. Qualitative characterization of the surface and sub-surface oxidized states of the samples

After the 170h-long stay in the furnace where they were in contact with the laboratory air at 1200°C the six samples get rather severely oxidized. A part of the oxides formed obviously spalled off during the cooling since some small oxides were found the ceramic shuttle of each of the alloys. These oxides were collected and subjected to X-ray diffraction. Two XRD diffractograms are shown as examples in Figure 2 (oxides having quitted the 1Co4NiTa alloy) and Figure 3 (coming from the 4Co1NiTa alloy). Obviously chromia was present, in all cases, in the parts of the

external scale having spalled off. A complex oxide of both chromium and tantalum, whose formula is CrTaO_4 , was also systematically found regardless of the considered alloy. Spinel oxides obviously also formed, NiCr_2O_4 for the Ni-richest alloy and CoCr_2O_4 for the alloys containing Co quantities high enough. NiO was also noted for the 0Co5NiTa alloy.

Other parts of the formed oxides, the ones having remained on the samples, were observed and identified during the SEM/BSE observation and the EDS spot analysis allowed by the prepared cross-sectional samples. Some illustrations given in Figure 4 allow seeing that the external oxides have quitted the alloys here and there, but the study of the remaining parts led to enrich the list of the oxide present, with notably the cobalt oxide CoO as well as various complex oxides for the 5Co0NiTa. All the observed oxide types are gathered per alloy in the lines of Table 2.

3.3. Quantitative characterization of the oxides

The parts of the external oxide scale remaining on the samples' surfaces were subjected to the measurement of their thicknesses. Except for the 0Co5NiTa alloy for which no surface oxide was available consequently to spallation at cooling or to accidental unhooking during handling before embedding, the parts of oxides remaining on the surfaces of the other samples were numerous enough to allow estimating the external scale thickness. Globally, from the 1Co4NiTa alloy to the 3Co2NiTa one, the average thickness of external oxide scale tends to increase when more and more cobalt was present in the alloys (Figure 5). Average thickness and standard deviation both suddenly increase when arriving to the two Co-richest alloys. For these alloys a part of surface was covered by mainly chromia while starting catastrophic oxidation led to

complex and thick mix of oxides in other locations. Internally, oxides of both chromium and tantalum appeared and grew in the sub-surface of the alloys. The depth of final presence of these internal oxides was measured, leading to the second curve plotted in Figure 5. Obviously, the CrTaO₄ depth of presence increases when Co replaces more and more Ni in the alloy. In the same way as the external oxidation, the CrTaO₄ depth becomes scattered for the two Co-richest alloys, with as results high average and standard deviation values.

3.4. Characterization of the changes in sub-surface: chemical changes

The development of a chromia scale and the formation of a significant quantity of CrTaO₄ oxide, externally as internally, has induced a decrease in Cr and Ta in the sub-surface, with as consequence threats for the chromia-forming behavior. In a first time the Cr content existing in extreme surface after the oxidation stage was specified by several EDS spot analyses in the alloy very close to the interface with the external oxide scale. This led to the first graph of Figure 6. One can see that, when the Co content in alloy increases, the Cr content in extreme surface decreases. This decrease is first slowly from the 0Co5NiTa alloy to the 3Co2NiTa one. The decrease accelerates when going to the 4Co1NiTa alloy (under 15wt.%Cr) and finally to the 5Co0NiTa one (around 7wt.%Cr). Notably with this last alloy one can understand that the loss of the chromia-forming behavior is probably imminent in some surface areas while catastrophic oxidation was already begun elsewhere.

The Ta content in extreme surface has also been measured and the results plotted in Figure 6. The minimal Ta content in extreme surface first decreases rapidly from a little more than 2.5wt.% when Co is added to the Ni-based alloy and this decrease slows

down when approaching the Co-based alloy, for which it is at an average low value close to 0.4wt.%.

In addition to the Cr content in extreme surface, the extent of the parts the parts of the alloys which were impoverished in chromium is of high importance to value the remaining potential of oxidation resistance of these alloys. The depths depleted in chromium were thus also measured. Obviously, after 170 hours at 1200°C in air the Cr-depleted zones of most alloys are about 400µm deep. The depths of Cr impoverishment of the 5Co0NiTa alloy is lower since close to 250µm.

These values were calculated from the measurements done on several concentration profiles per alloy. An example per alloy is given in Figure 8 for Cr, and in Figure 9 for Ta. It appears that a major part of the decrease in Cr or in Ta when coming from the bulk and going to the external surface is rather linear. After having selected the profiles displaying linear parts not too perturbed by the presence of internal oxides or carbides, visible (intersected by the cross section) or not (existing just under the cutting plane), the slope of these linear parts were determined. The obtained values are presented as graph in Figure 10. Obviously the Cr gradient increases when the Co content increases (it can be particularly high for the alloy containing only cobalt). This is also the case of the Ta gradient which increases more regularly with the Co content in alloy.

3.5. Characterization of the changes in sub-surface: microstructure changes

The micrographs displayed in Figure 11 are enlarged views of the sub-surfaces at the same locations on the samples as in Figure 4. One can note that carbides have disappeared from the external surface, to a depth which decreases when the Co content in alloy increases. Two types of carbide-free depths are to consider: the ones of

disappearance of the chromium carbides specifically, and the ones of TaC disappearance. The Cr₇C₃-free depth and the TaC-free one are plotted together in Figure 12. No significant difference exists between the two alloys containing chromium carbides at 1200°C: the Cr₇C₃-free depth stays around 370μm for both alloys. In contrast, the depth of TaC disappearance, which concerns all alloys, regularly decreases when more and more cobalt is present in the alloy (from 250 to 100μm, typically).

3.6. Microstructure changes and consequences for hardness

The microstructures in the bulk of the oxidized alloys are more or less different from the initial ones (Figure 13). Changes are particularly important for the Ni-richest alloys: the chromium carbides as well as the tantalum carbides have both become round in the 0Co5NiTa alloy. The same effect is found for the chromium carbides in the 1Co4NiTa alloy while the initial script-like shape of the TaC is a little kept although a fragmentation phenomenon occurred for them. This also happened for the TaC carbides of the four other alloys which are totally free of chromium carbides. This is new for the 2Co3NiTa and 3Co2NiTa alloys while such carbides did not exist in the as-cast microstructures of the two Co-richest alloys.

By seeing these morphological modifications of the carbides networks one can imagine a decrease in room temperature hardness of the alloys by comparison with the as-cast state. Such effect was obviously not systematically encountered, as shown by the graphs in Figure 14. One can just notice that the logical increase in hardness from the 0Co5NiTa alloy to the 5Co0NiTa one is more regular for the aged alloys than for the as-cast ones.

4. Discussion

The persistence of chromium carbides in a nickel-chromium alloy though chemically designed to contain only tantalum carbides by the choice of equal atomic contents for tantalum and carbon, not expected because of the standard formation free enthalpy of TaC which is much lower than the chromium carbides ones [25], was observed again. Despite the chromium content 5wt.%-lower than the cast Ni-30Cr-0.4C-6Ta alloy earlier study [24], chromium carbides still compete with tantalum carbides. This is not only due to non-equilibrium reasons since the chromium carbides remained present during the 1200°C stage. This is also true for the 1Co4NiTa alloy. Obviously, for 25wt.%Cr in the alloy, at least 27-28wt.% of cobalt is compulsory to obtain the wished microstructure containing only TaC. While the morphology of the chromium carbides considerably evolves at 1200°C, the script-like shape of the tantalum carbides suffer only moderate changes (fragmentation but not coalescence as the chromium carbides).

Concerning the oxidation behavior, containing only two high oxidable elements – Cr and Ta – but also Ni and especially cobalt, two elements able to take part in the formation of spinel oxides, the corrosion products formed by oxidation at 1200°C are numerous. Fortunately Cr₂O₃ stays the main specie in the external continuous oxide scales, allowing good resistance against hot oxidation. But oxides associating chromium and tantalum also form systematically (CrTaO₄), as constituent of the external scale and as internal oxide. Even if chromia is also present internally, CrTaO₄ is the major internal oxide. Knowing the good behavior of Cr-rich Ni-based binary [26] and Ni-Cr-C alloys [27], not only in isothermal oxidation but also in cyclic oxidation (resistance of the formed chromia against spallation), the loss of significant parts of the oxide scales by the samples studied here despite low cooling rates (cooling lower than in [26, 27],

one can attribute to tantalum and to CrTaO₄ this oxide spallation at cooling. Indeed this internal oxide is mainly present close to the interface and it can be thought that it inhibits the good adherence of chromia to the nude metallic alloy.

Involved in great quantities in the oxidation phenomena, chromium and tantalum have significantly quitted the alloys. The zone which is the most affected by this migration toward the growing external oxide scale (especially Cr) and to the outermost internal oxides (essentially Ta) is logically the sub-surface. Certainly from the alloy surface towards the bulk a zone impoverished in Cr and in Ta developed, these local changes in chemical composition destabilizing the corresponding carbides (either Cr_xC_y and Ta, or only TaC, depending on the considered alloys) with as results their decomposition and the outward diffusion of their respective constituting elements.

As suggested by several metallography observations:

- depth of carbide-free zones which decreases when more and more cobalt is present in alloy,

and local chemical analyses:

- Cr and Ta contents in extreme surface which both decrease when more and more cobalt is present in alloy
- Cr-depleted depth decreasing at the same time
- Cr and Ta concentration gradients both stronger and stronger

diffusion seems more and more difficult for the two elements. Obviously, the presence of more and more cobalt in the matrix is detrimental for the mobility of Cr and for Ta. This is well-known for chromium and this is one of the principal reasons of the

low resistance of cobalt-based alloys by comparison to the nickel-based-ones. But the effect on Ta diffusion is maybe not so well known.

Here the hindering effect of Co on Cr diffusion threatened the chromium supply of the oxidation front, with as consequences the difficulty for maintaining the Cr content in extreme surface at a level staying high enough to sustain the chromia-forming behavior. The loss of this favorable behavior leading to local catastrophic oxidation in the case of the 5Co0NiTa alloy is to attribute to the Cr content become lower than 5wt.%Cr in some areas. Concerning Ta, its hampered diffusion due to cobalt was rather a positive effect for the subsurface mechanical strengthening: TaC did not disappeared too deeply. This can be important for flexural solicitations since this induces tensile stress parallel to the external surface and concentrated close to this surface where carbides are thus no longer present, but not for tensile solicitations because of the low proportion of carbide-less alloy in the piece thickness, except if this one is particularly thin.

To summarize one can say, in this {Co and/or Ni}-25Cr-0.4C-6Ta system, that it is not possible to gather the best mechanical behavior and the best oxidation behavior, both at high temperature, in the same alloy of this family. The Ni-richest alloys are the most oxidation resistance (protective chromia scale) but probably the worst mechanically resistant (total loss of the initial acicular or script morphologies of the Cr and Ta carbides respectively) as suggested by their rather soft result to Vickers indentation at room temperature. The Co-richest alloys present potential good mechanical properties at high temperature (TaC carbides only, with script-like morphology not too heat-affected, high level of room temperature hardness) but more or

less threatened by catastrophic oxidation because of hindered diffusion of the key element Cr).

5. Conclusion

The nature and high temperature mechanical role of the interdendritic population of primary carbides and the easiness of the oxidation front Cr supply are both governed by the {Ni, Co}-balance sheet of the matrix. Unfortunately, among superalloys with chemical compositions close to the simple ones studied here, a choice must be done between good mechanical resistance and good oxidation resistance. In service, moderate stresses but very aggressive atmospheres will lead to the Ni-richest versions while the inverse situation will lead to the Co-richest versions. Because of the obvious too preoccupant problem of oxide spallation of the Ni-richest alloys conferred by tantalum which diffuses too fast and forms high quantity of sub-areaal CrTaO₄ oxides obviously detrimental to chromia adherence, unacceptable in case of thermal-cycling conditions, only the alloys containing cobalt with content high enough are really interesting for developing optimized TaC-reinforced chromia-forming cast superalloys. For instance, for long use at temperatures close to 1200°C, these are possibly the 3Co2NiTa (28wt.%Ni) and 4Co1NiTa (14wt.%Ni) alloys which are the most interesting alloys from which it is possible to extrapolate operational alloys. Indeed they appear tentatively as the best compromise for all properties, before additional oxidation tests and real mechanical tests.

References

- [1] M. J. Donachie and S. J. Donachie: “Superalloys – A technical guide (2nd ed.)”; 2002, Materials Park, ASM International.
- [2] C. T. Sims, W. C. Hagel: “The Superalloys”; 1972, New York, John Wiley & Sons.
- [3] P. Berthod: Looking for new polycrystalline MC-reinforced cobalt-based superalloys candidate to applications at 1200°C. *Advances in Materials Science and Engineering*, 2017, open access article ID 4145369
- [4] E. Conrath, P. Berthod: Properties of a HfC-reinforced nickel-based superalloy in creep and oxidation at 1100°C. *Materials Science*, 2018, 53, 6, 861-867.
- [5] S. Michon, P. Berthod, L. Aranda, C. Rapin, R. Podor and P. Steinmetz: Application of thermodynamic calculations to study high temperature behavior of TaC-strengthened Co-base superalloys. *Calphad*, 2003, 27, 289-294.
- [6] P. Berthod, S. Michon, L. Aranda, S. Mathieu, J. C. Gachon: Experimental and thermodynamic study of the microstructure evolution in cobalt-base superalloys at high temperature. *Calphad*, 2003, 27, 353-359.
- [7] W. Gui, X. Zhang, H. Zhang, X. Sun, Q. Zheng: Melting of primary carbides in a cobalt-base superalloy. *Journal of Alloys and Compounds*, 2019, 787, 152-157.
- [8] Z. Opiekun: Influence of zirconium and heat treatment on the structure of heat-resistant cobalt casting alloys of Mar-M509 type. *Journal of Materials Science*, 1987, 22, 5, 1547-1556.
- [9] P. Berthod, J.-L. Bernard, C. Liébaud: Cobalt based alloy, article made from said alloy and method for making same. *PCT Int. Appl.* (1998), WO 99/16919.

- [10] P. Berthod, J.-L. Bernard, C. Liébaut: Cobalt-chromium alloy for spinner cups in manufacture of mineral wool from silicate glass. *PCT Int. Appl.* (2001), WO 2001090429.
- [11] M. Montazeri, F. M. Ghaini, A. Farnia: An investigation into the microstructure and weldability of a tantalum-containing cast cobalt-based superalloy. *International Journal of Material Research*, 2011, 102, 1446-1451.
- [12] W. V. Youdelis and O. Kwon: 'Carbide phases in cobalt base superalloy: role of nucleation entropy in refinement', *Mater. Sci.*, 1983, 17, 379-384.
- [13] W. V. Youdelis, O. Kwon: Carbide phases in nickel-base superalloy: nucleation properties of MC type carbide. *Metal Science*, 1983, 17, 8, 385-388.
- [14] G. M. Janowski, R. W. Heckel, B. J. Pletka: The effect of tantalum on the microstructure of two polycrystalline nickel-base superalloys: B-199 + Hf and MAR-M247. *Metallurgical Transactions A: Physical Metallurgy and Materials Science*; 1986, 17A, 11, 1891-1905.
- [15] G. M. Janowski, B. S. Harmon, B. J. Pletka: Thermal stability of the nickel-base superalloy B-1900 + Hf with tantalum variations. *Metallurgical Transactions A: Physical Metallurgy and Materials Science*; 1987, 18A, 8, 1341-1351.
- [16] L. Zheng, G. Zhang, T. L. Lee, M. J. Gorley, Y. Wang, C. Xiao, Z. Li: The effects of Ta on the stress rupture properties and microstructural stability of a novel Ni-base superalloy for land-based high temperature applications. *Materials & Design*, 2014, 61, 61-69.
- [17] S. Gao, J. Hou, F. Yang, Y. Guo, C. Wang, L. Zhou: Effects of tantalum on microstructure and mechanical properties of cast IN617 alloy. *Materials Science &*

Engineering A: Structural Materials: Properties, Microstructures and Processing, 2017, 706, 153-160.

[18] D. A. Woodford: Creep and rupture of an advanced fiber strengthened eutectic composite superalloy. *Metallurgical Transactions A: Physical Metallurgy and Materials Science*, 1977, 8A, 4, 639-650.

[19] E. R. Buchanan, L. A. Tarshis: Strengths and failure mechanisms of a cobalt-chromium-tantalum carbide (Co-15Cr-13TaC) directionally solidified eutectic alloy. *Metallurgical Transactions*, 1974, 5, 6, 1413-1422.

[20] R. Gilles, D. Mukherji, L. Karge, P. Strunz, P. Beran, B. Barbier, A. Kriele, M. Hofmann, H. Eckerlebe and J. Roesler: ‘Stability of TaC precipitates in a Co-Re-based alloy being developed for ultra-high temperature applications’, *J. Appl. Cryst.*, 2016, 49, 1253-1265.

[21] L. Karge, R. Gilles, D. Mukherji, P. Strunz, P. Beran, M. Hofmann, J. Gavilano, U. Keiderling, O. Dolotko, A. Kriele, A. Neubert, J. Roesler and W. Petry: The influence of C/Ta ratio on TaC precipitates in Co-Re base alloys investigated by small-angle neutron scattering, *Acta Materialia*, 2017, 132, 354-366.

[22] P. Kofstad: “High temperature corrosion”; 1988, London, Elsevier applied science.

[23] D. J. Young: “High temperature oxidation and corrosion of metals”; 2008, Amsterdam, Elsevier.

[24] P. Berthod, L. Aranda, C. Vébert, S. Michon: Experimental and thermodynamic study of the high temperature microstructure of tantalum containing nickel-based alloys. *Calphad*, 2004, 28, 159–166.

[25] S. R. Shatynski: The thermochemistry of transition metal carbides. *Oxidation of Metals*, 1979, 13(2), 105-118.

[26] P. Berthod: Kinetics of high temperature oxidation and chromia volatilization for a binary Ni–Cr alloy. *Oxidation of Metals*, 2005, 64(3/4), 235-252.

[27] P. Berthod: Influence of chromium carbides on the high temperature oxidation behavior and on chromium diffusion in nickel-base alloys. *Oxidation of Metals*, 2007, 68, 77-96.

FIGURES

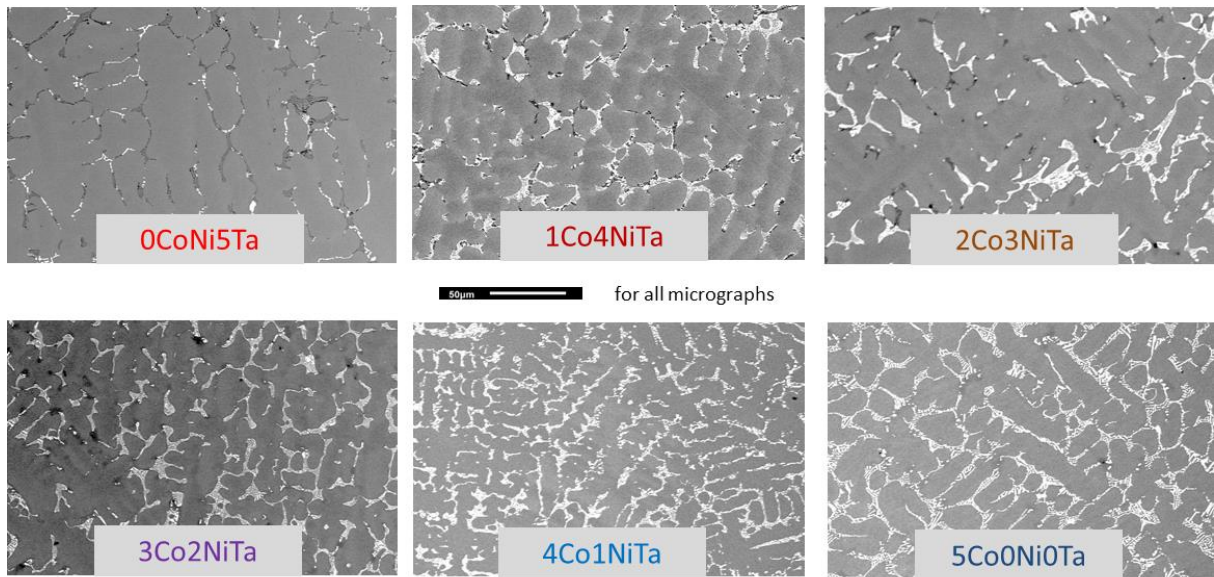


Fig. 1. SEM/BSE micrographs illustrating the as-cast microstructures of the six studied alloys (magnification: $\times 250$)

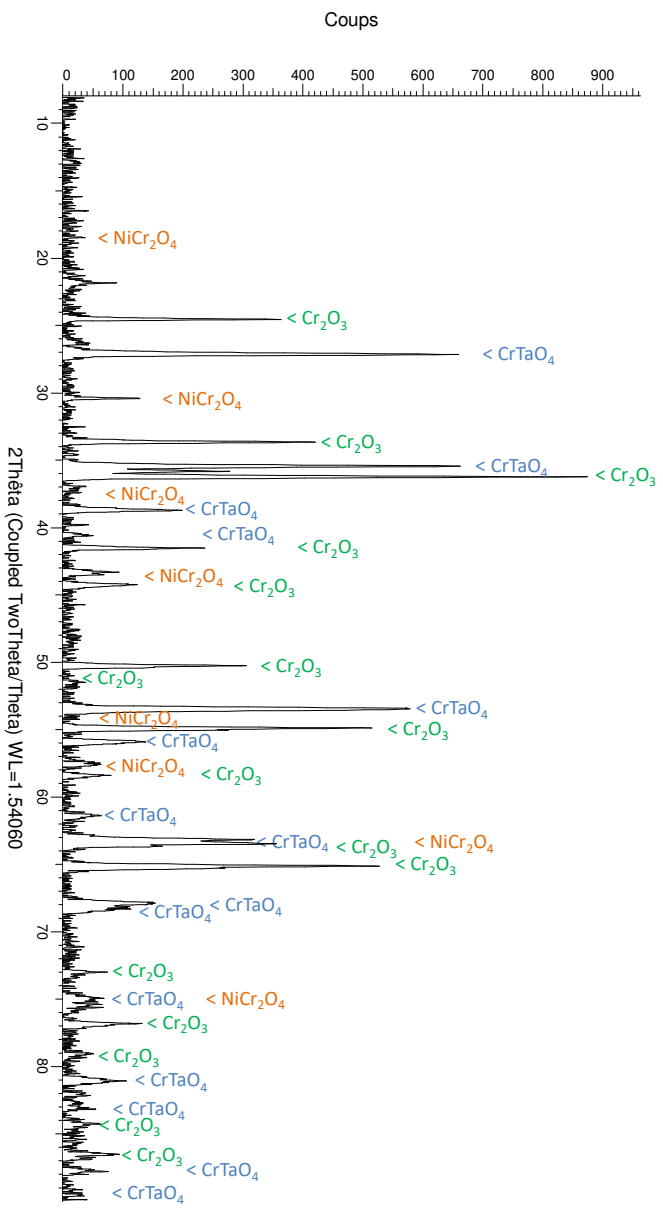


Fig. 2. Diffractogram resulting from the XRD analysis of the oxides spalled off during the post-isothermal stage cooling of the 1Co4NiTa alloy

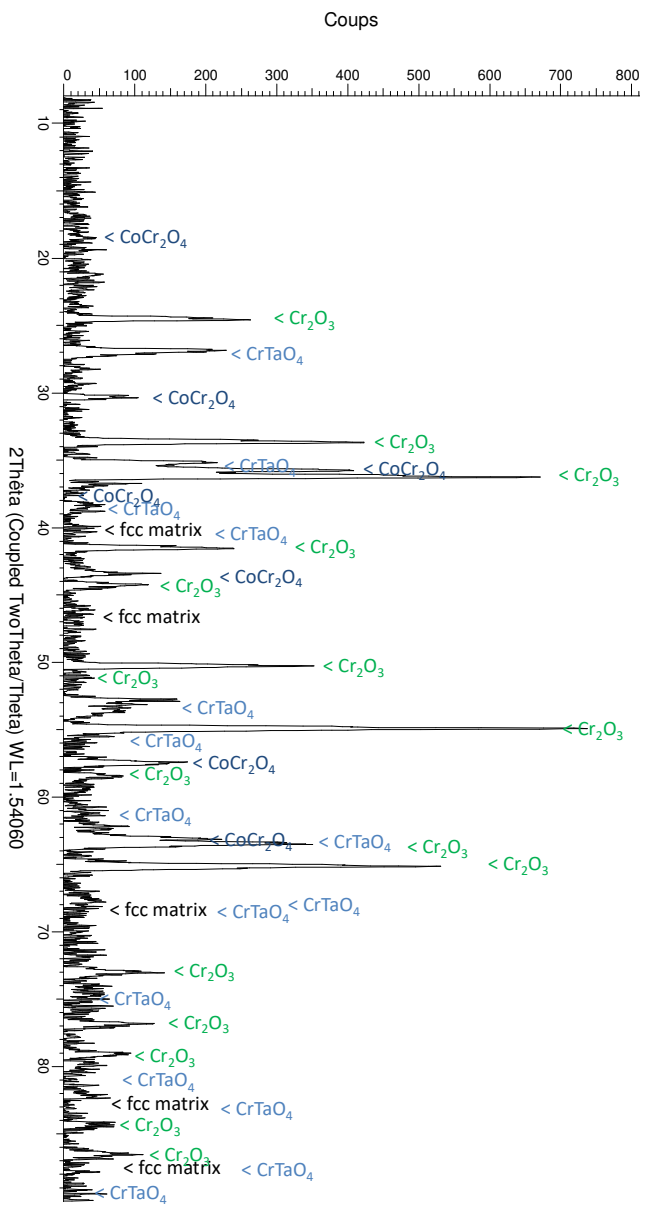


Fig. 3. Diffractogram resulting from the XRD analysis of the oxides spalled off during the post-isothermal stage cooling of the 4Co1Ni1Ta alloy

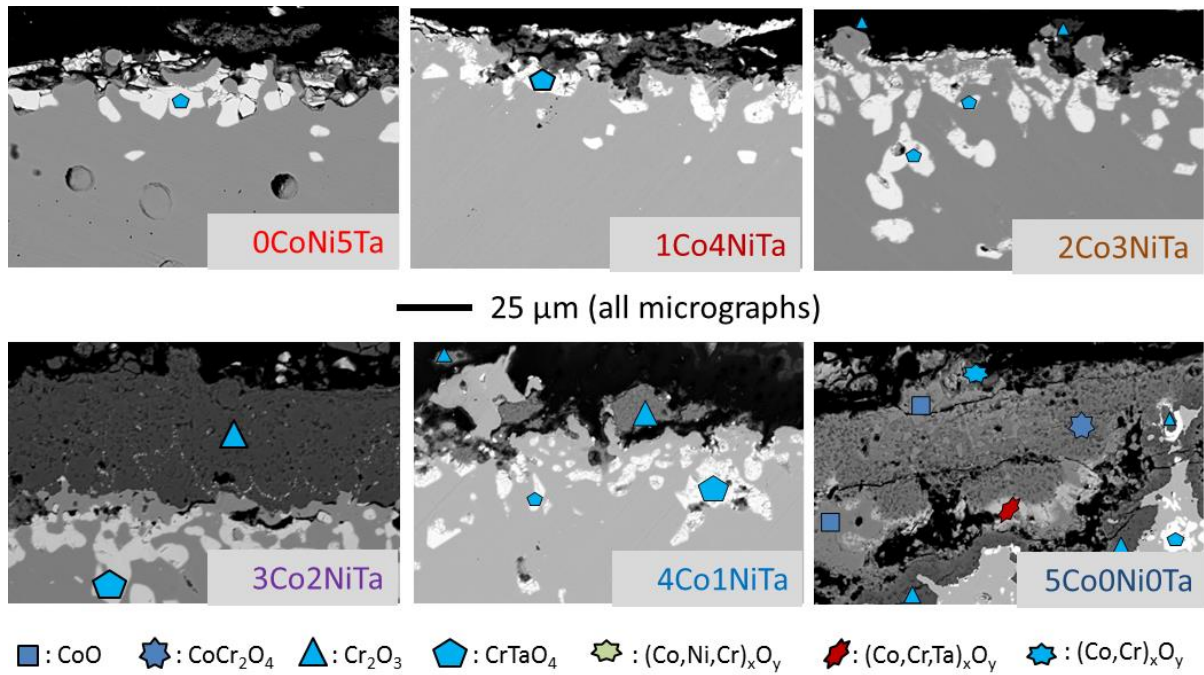


Fig. 4. SEM/BSE micrographs illustrating the surface and sub-surface oxidized states of the six studied alloys

(magnification: ×1000)

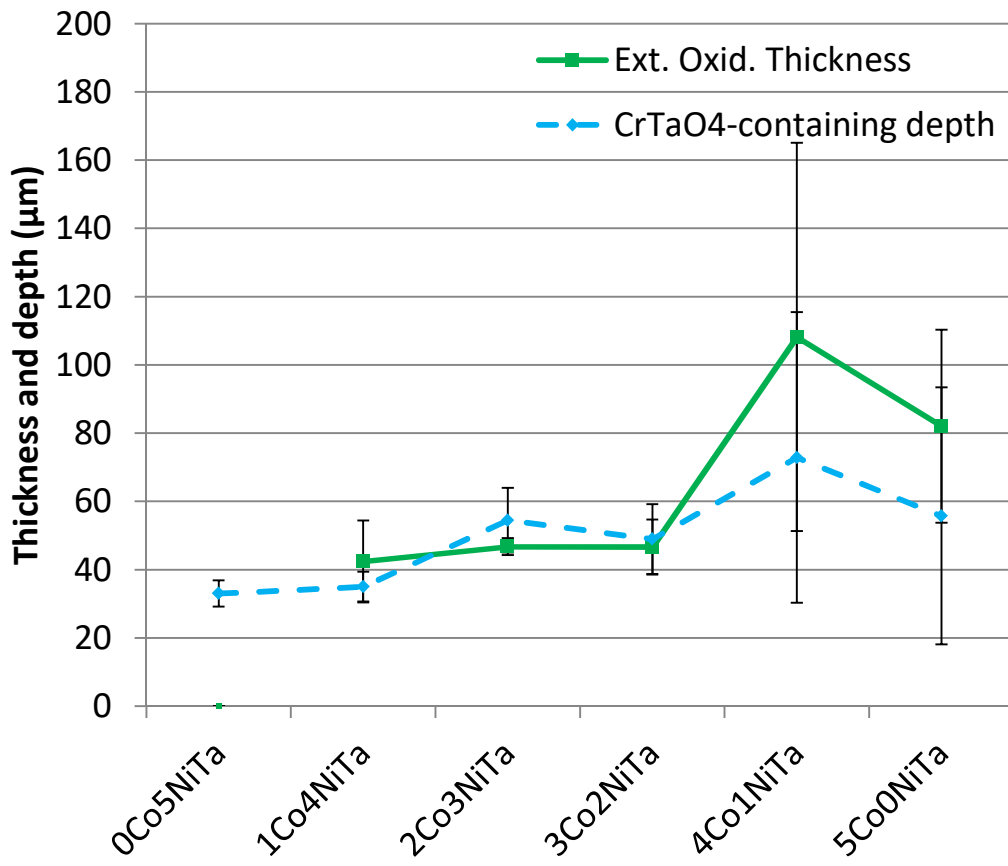


Fig. 5. Thicknesses of the Cr_2O_3 parts remaining on surface and depths of presence of the complex internal CrTaO_4 oxides

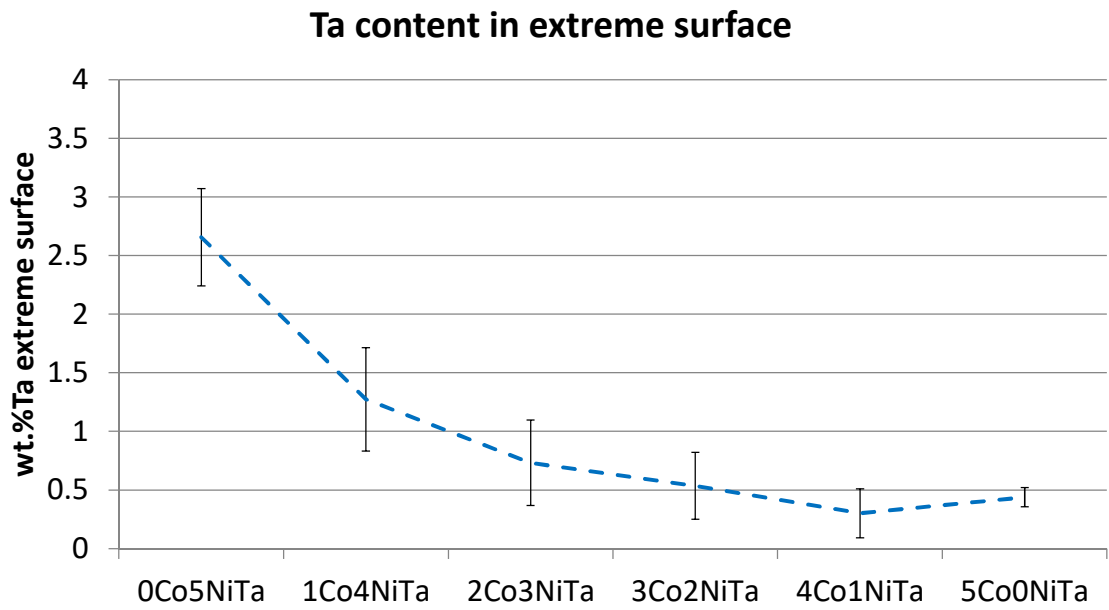
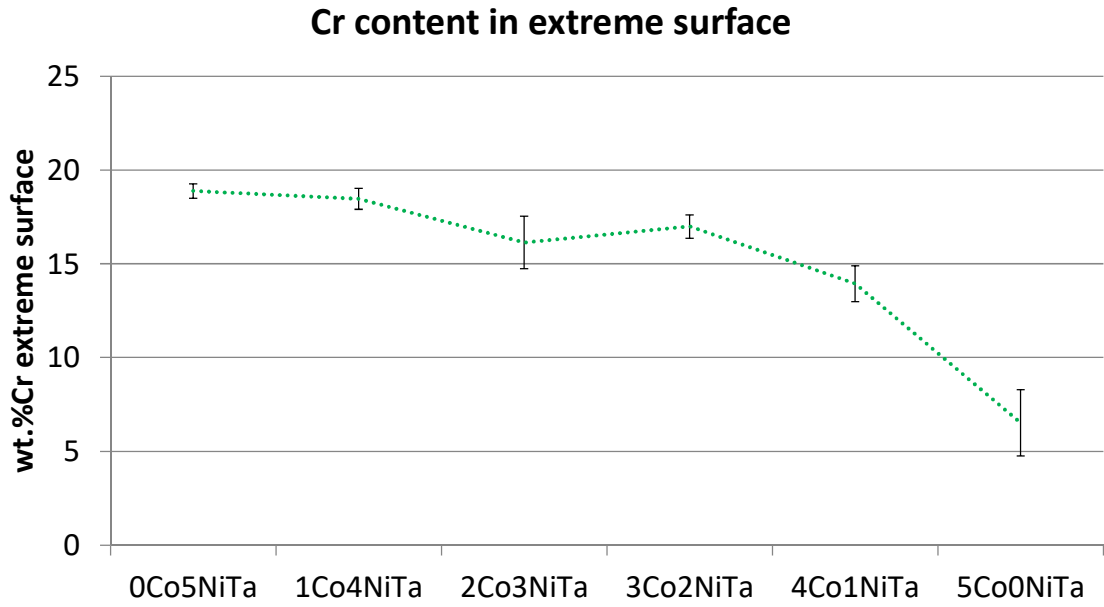


Fig. 6. Cr (top) and Ta (bottom) weight contents in extreme surface of the oxidized samples, plotted versus the Co/Ni ratio of the alloy

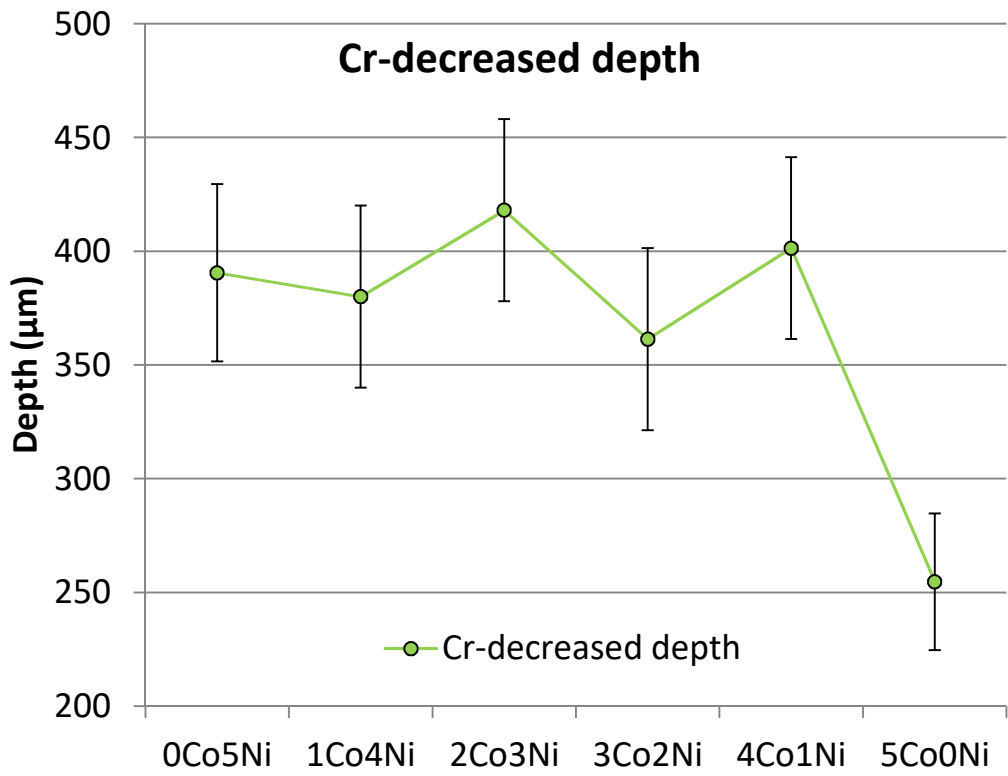


Fig. 7. Cr-depleted depth in the sub-surface of the oxidized samples, plotted versus the Co/Ni ratio of the alloy

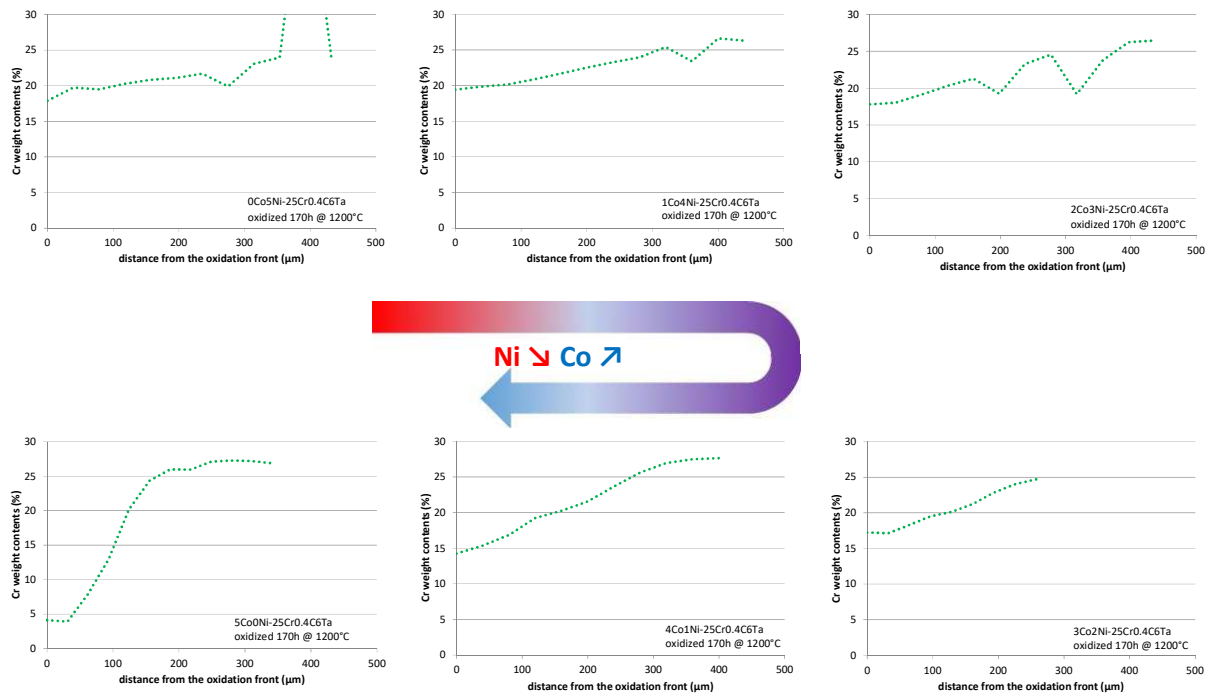


Fig. 8. Cr concentration profiles in the sub-surfaces of the six oxidized samples

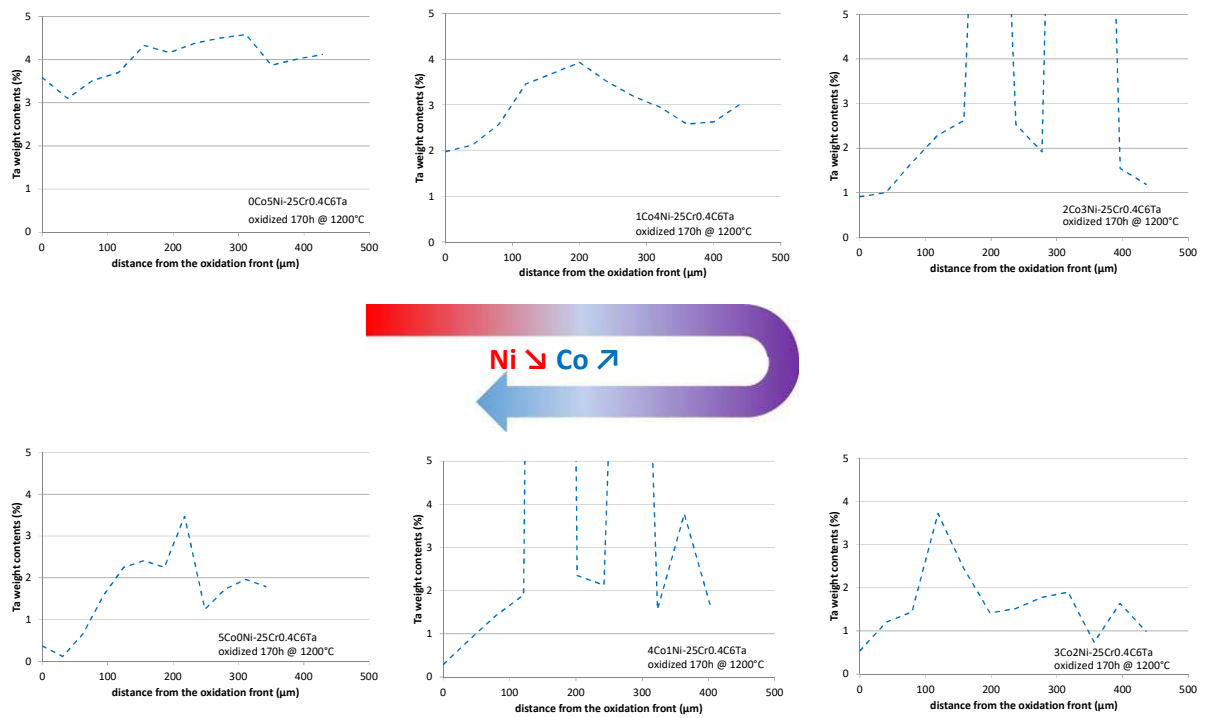


Fig. 9. Ta concentration profiles in the sub-surfaces of the six oxidized samples

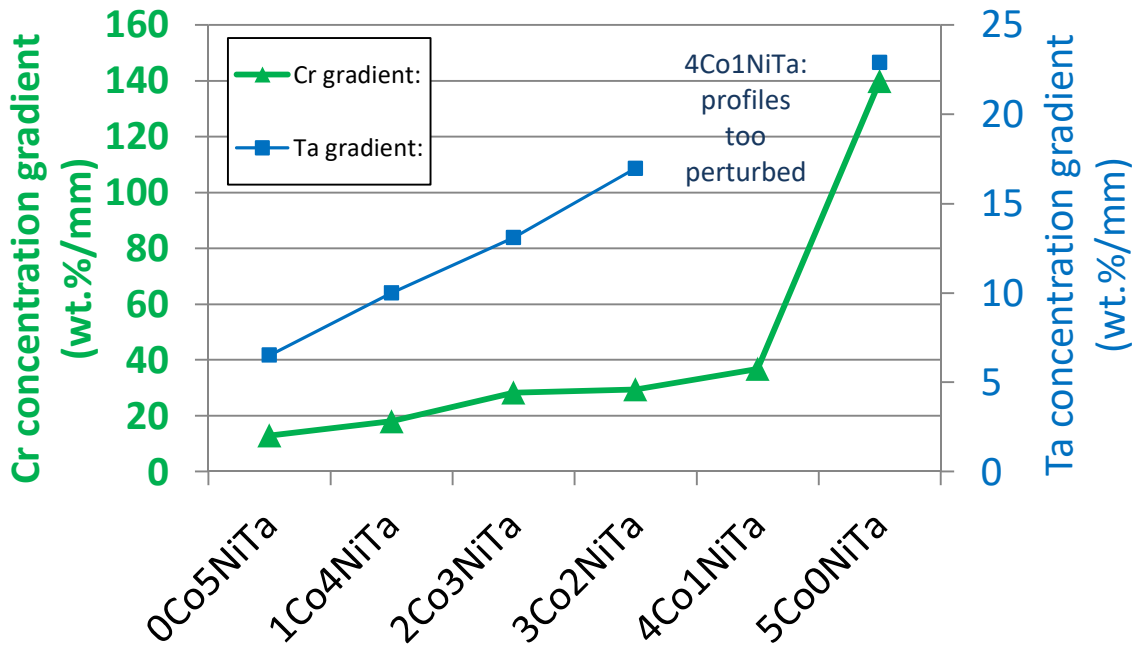


Fig. 10. Values of the Cr and Ta concentration gradients in the sub-surfaces of the oxidized samples, plotted versus the Co/Ni ratio of the alloy

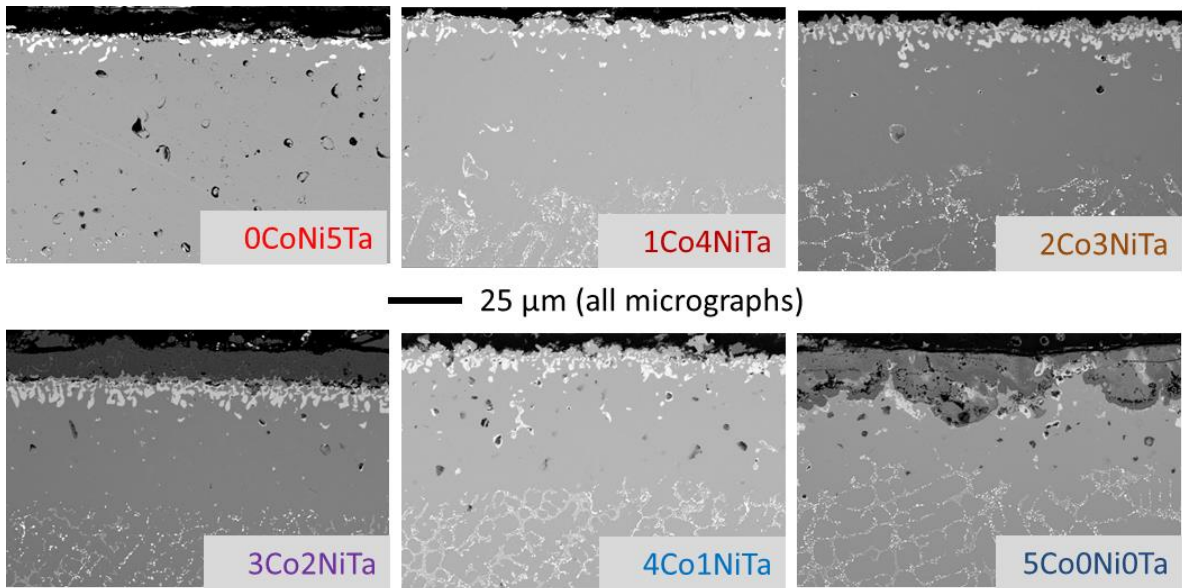


Fig. 11. SEM/BSE micrographs showing the disappearance of the carbides in the sub-surface of the six oxidized alloys

(magnification: $\times 250$)

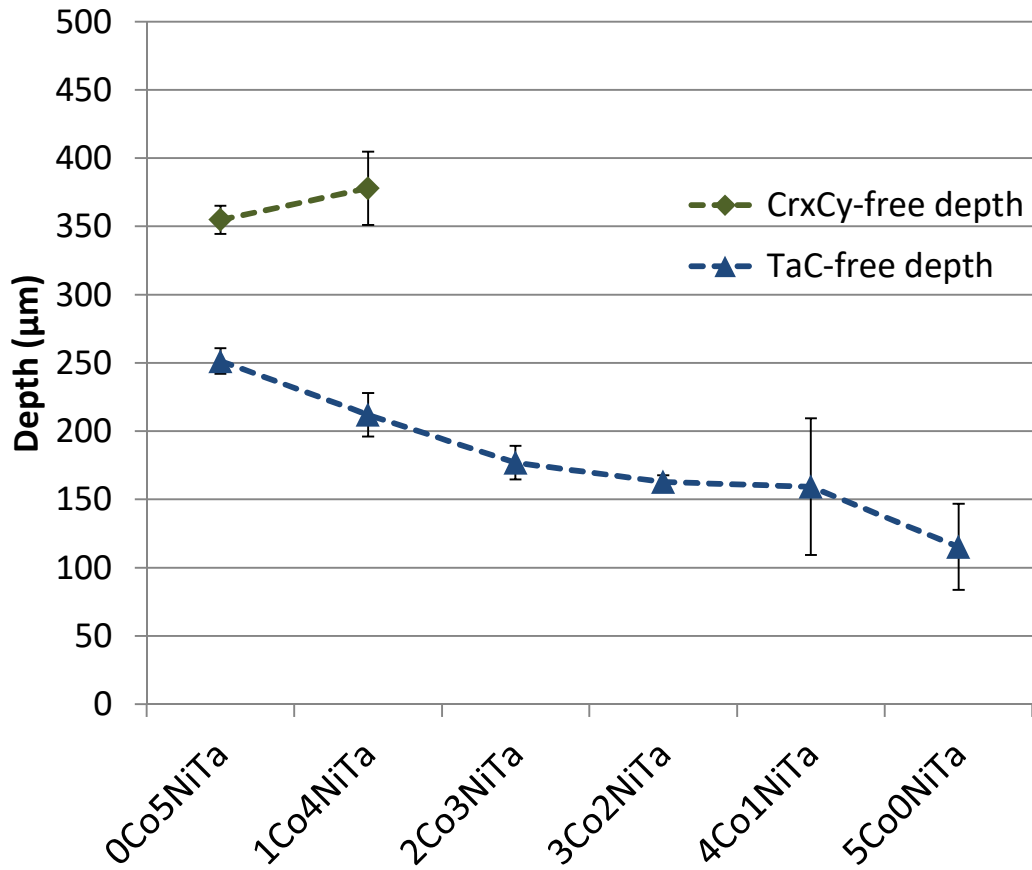


Fig. 12. Carbides-free depths (disappearance of either CrxCy or TaC) in the sub-surfaces of the oxidized samples, plotted versus the Co/Ni ratio of the alloy

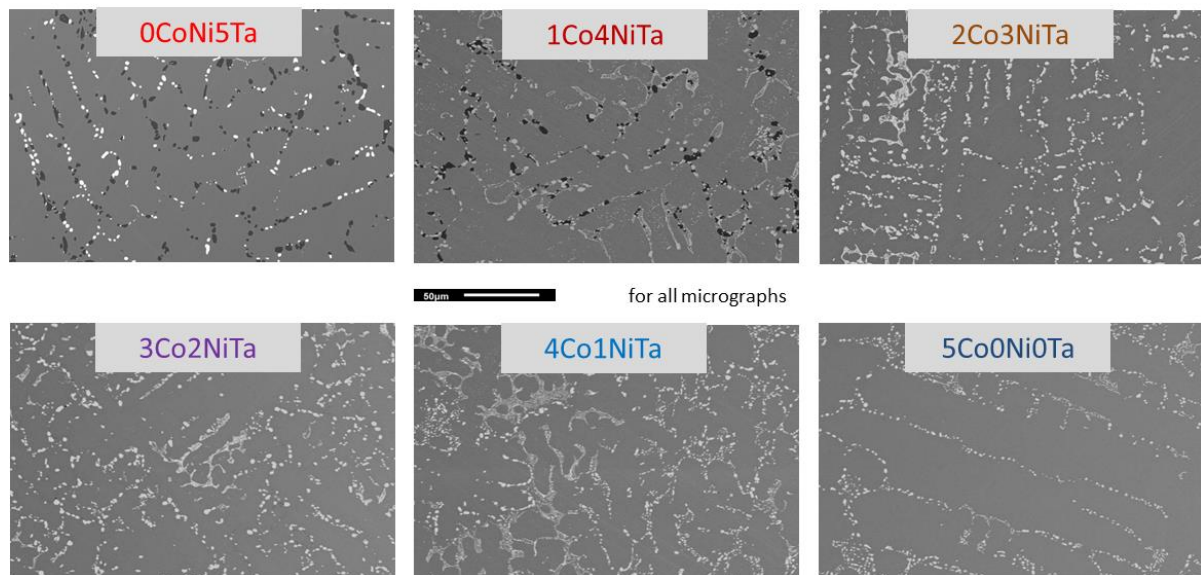


Fig. 13. SEM/BSE micrographs illustrating the {170h, 1200°C}-aged microstructures of the six studied alloys (magnification: $\times 250$)

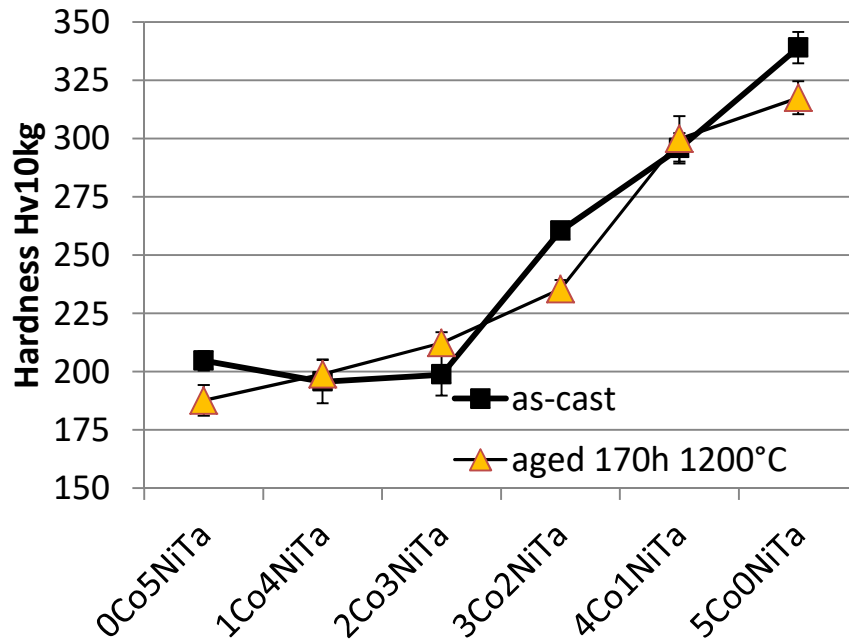


Fig. 14. Vickers hardness (average and standard deviation values from ten measurements) in the bulk of the oxidized samples, plotted versus the Co/Ni ratio of the alloy

TABLES

Table 1: Chemical compositions of the six studied alloys (average and standard deviation values from five $\times 250$ full frame EDS measurements)

wt.%	M (*: Co, **:Ni)	Cr	Ta
0Co5NiTa	0*	25.3 \pm 0.2	6.7 \pm 0.3
1Co4NiTa	13.9 \pm 0.1*	25.8 \pm 0.2	6.5 \pm 0.2
2Co3NiTa	27.6 \pm 0.1*	25.3 \pm 0.3	6.5 \pm 0.3
3Co2NiTa	25.6 \pm 0.3**	25.6 \pm 0.1	6.9 \pm 0.1
4Co1NiTa	12.6 \pm 0.4**	26.1 \pm 0.7	5.8 \pm 1.7
5Co0NiTa	0**	25.6 \pm 0.1	7.2 \pm 0.2

Table 2: Summary of the oxides present on the oxidized surfaces of the six alloys, according to XRD, SEM/BSE imaging and SEM/EDS measurements

wt.%	M (*: Co, **:Ni)	Cr	Ta
0Co5NiTa	0*	25.3 ±0.2	6.7 ±0.3
1Co4NiTa	13.9 ±0.1*	25.8 ±0.2	6.5 ±0.2
2Co3NiTa	27.6 ±0.1*	25.3 ±0.3	6.5 ±0.3
3Co2NiTa	25.6 ±0.3**	25.6 ±0.1	6.9 ±0.1
4Co1NiTa	12.6 ±0.4**	26.1 ±0.7	5.8 ±1.7
5Co0NiTa	0**	25.6 ±0.1	7.2 ±0.2